AGU PUBLICATIONS

Water Resources Research

RESEARCH ARTICLE
10.1002/2017WR020778

Key Points:
- Atmospheric rivers contribute to up to 60% total winter precipitation and up to 64%/72% extreme daily precipitation in Salt/Verde river basins
- Warmer than normal temperatures during atmospheric river landfallings linked to higher melting lines and to rain-on-snow processes
- Atmospheric rivers generate 43% of the annual maximum flows in inland basins in Arizona

Supporting Information:
- Supporting Information S1
- Figure S1
- Figure S2
- Figure S3
- Figure S4
- Figure S5
- Figure S6
- Figure S7
- Figure S8

Correspondence to:
E. M. C. Demaria,
eleonora.demaria@ars.usda.gov

Citation:
Demaria, E. M. C., Dominguez, F., Hu, H., von Glinski, G., Robles, M., Skindlov, J., & Walter, J. (2017). Observed hydrologic impacts of landfalling atmospheric rivers in the Salt and Verde river basins of Arizona, United States. *Water Resources Research*, *53*. https://doi.org/10.1002/2017WR020778

Received 16 MAR 2017
Accepted 4 OCT 2017
Accepted article online 9 OCT 2017

Observed Hydrologic Impacts of Landfalling Atmospheric Rivers in the Salt and Verde River Basins of Arizona, United States

Eleonora M. C. Demaria[1], Francina Dominguez[2], Huancui Hu[2], Gerd von Glinski[3], Marcos Robles[4], Jonathan Skindlov[5], and James Walter[5]

[1]USDA-ARS, Southwest Watershed Research Center, Tucson, AZ, USA, [2]Department of Atmospheric Sciences, University of Illinois at Urbana-Champaign, Urbana, IL, USA, [3]White Mountain Apache Tribe, Water Resources Program, Fort Apache, AZ, USA, [4]The Nature Conservancy, Tucson, AZ, USA, [5]Salt River Project, Phoenix, AZ, USA

Abstract Atmospheric rivers (ARs), narrow atmospheric water vapor corridors, can contribute substantially to winter precipitation in the semiarid Southwest U.S., where natural ecosystems and humans compete for over-allocated water resources. We investigate the hydrologic impacts of 122 ARs that occurred in the Salt and Verde river basins in northeastern Arizona during the cold seasons from 1979 to 2009. We focus on the relationship between precipitation, snow water equivalent (SWE), soil moisture, and extreme flooding. During the cold season (October through March) ARs contribute an average of 25%/29% of total seasonal precipitation for the Salt/Verde river basins, respectively. However, they contribute disproportionately to total heavy precipitation and account for 64%/72% of extreme total daily precipitation (exceeding the 98th percentile). Excess precipitation during AR occurrences contributes to snow accumulation; on the other hand, warmer than normal temperatures during AR landfallings are linked to rain-on-snow processes, an increase in the basins' area contributing to runoff generation, and higher melting lines. Although not all AR events are linked to extreme flooding in the basins, they do account for larger runoff coefficients. On average, ARs generate 43% of the annual maximum flows for the period studied, with 25% of the events exceeding the 10 year return period. Our analysis shows that the devastating 1993 flooding event in the region was caused by AR events. These results illustrate the importance of AR activity on the hydrology of inland semiarid regions: ARs are critical for water resources, but they can also lead to extreme flooding that affects infrastructure and human activities.

Plain Language Summary Within the Salt and Verde River basins in the semiarid northeastern Arizona, natural ecosystems and humans compete for over-allocated water resources. The basins are highly dependent on winter precipitation for ecosystem functioning, water supply, fire suppression, and in the case of extreme events, for water quality, flood control and dam safety. Atmospheric Rivers (ARs) are narrow corridors of concentrated water vapor that bring copious amount of rainfall from the Pacific into the region and contribute to its hydrology by increasing snow pack and replenishing soil moisture in the basins. ARs are also responsible for extreme precipitation and streamflow events, such as the 1993 flooding event, which caused human casualties and economic losses. These results illustrate the importance of AR activity on the hydrology of inland semiarid regions: ARs are critical for maintaining natural ecosystem health, but they can also lead to extreme flooding that affects infrastructure and human activities.

1. Introduction

Past studies have focused on the hydrometeorological impacts of narrow water vapor corridors called Atmospheric rivers (ARs) along the West Coast of the United States (Guan et al., 2013, 2016; Neiman et al., 2011; Ralph et al., 2006, 2013). In this region, a large portion of cool-season precipitation depends on a small number of AR events (Rutz et al., 2014). In California, landfalling ARs contribute to 30%–45% of the overall precipitation. These ARs are critical for water resources (Dettinger et al., 2011) and also are associated with the abrupt ending of droughts (Dettinger, 2013). While ARs are linked to extreme flooding along coastal areas (Neiman et al., 2011; Ralph et al., 2006, 2013), at higher elevations in the Sierra Nevada Mountains,

they are associated with up to four times more snowpack accumulation than non-AR storms, with the occurrence of rain-on-snow processes, and with larger streamflows (Guan et al., 2010, 2016).

Not only ARs are important along the Pacific coast, they also penetrate the intermountain southwestern U.S. and significantly contribute to the hydrometeorology of Arizona. Most of these ARs cross the Baja California Peninsula, interact with its topographical features, and then impinge on Arizona's Mogollon Rim, an escarpment that raises to approximately 2,400 m and defines the southwestern edge of the Colorado Plateau (Hughes et al., 2014; Rutz et al., 2014). Even though major topographic barriers contribute to the depletion of water vapor transported inland, the ARs can still enter the continent south of the higher mountains on the Baja peninsula, cross the Gulf of California, and reach Arizona, where they produce copious precipitation (Hughes et al., 2014). Rutz and Steenburgh (2012) showed that the inclusion of ARs from the southern tip of the Baja California Peninsula increases the percentage of cool-season (November–April) precipitation and snow in Arizona.

The Salt and Verde river basins (SVRB), located in the northeastern part of Arizona south of the Mogollon Rim, receive much of their winter precipitation from the interaction between these southwesterly ARs and the rugged terrain. The SVRB jointly cover an area of approximately 28,212 km^2 of midelevation mountain ranges and valleys. The elevation gain in the basins is approximately 3,332/3,109 m from the lowest point for the Salt/Verde river basins, respectively. The vegetation changes with elevation, from semidesert scrub to subalpine conifer forest. Precipitation is bimodal. Convective monsoonal rainfall in the summer months often evaporates quickly, though in many instances these high intensity-highly localized storms generate extreme flooding events (Hawkins et al., 2015). Winter precipitation on the other hand, accumulates as snow in higher elevations and contributes to spring runoff (Figures 1b and 1c).

In the SVRB, ARs are responsible for 25% of total cool-season precipitation (Rutz et al., 2014); however, they also contribute disproportionately to heavy precipitation events (Rivera et al., 2014) that can have significant societal impacts in the region (House & Hirschboeck, 1997). Extreme precipitation events associated with ARs can often lead to flooding, as was the case with the 27–28 January 2008 AR event in which flood waters rose above the tops of the Bootleg and Colley Dams (White Mountain Apache Tribe, personal communication, 2016). Neiman et al. (2013) analyzed an AR event that impinged upon Arizona on January 2010, which showed exceptionally strong Integrated Water Vapor (IWV) from the southwest, bringing warm air advection that resulted in heavy orographic precipitation, increases in snowpack, and flooding in northeastern Arizona.

With a population of over four million people, the Phoenix metro area in Arizona is the sixth largest metropolis in the United States; it is estimated that by the year 2030 the population will exceed six million (http://www.census.gov). The SVRB (Figure 1) contribute to approximately 93% of the Phoenix metro area's annual water supply, approximately 2,837 million m^3, drawn from a system of six reservoirs that store snowmelt runoff resulting from winter precipitation (Svoma, 2011), while the remaining 7% is provided by groundwater (Simonit et al., 2015). The basins are also important for two Native American tribes that rely heavily on the basins' natural resources for their livelihood and for numerous wilderness areas. For these reasons, assessments of AR events are crucial in the semiarid Southwest, where human and natural ecosystems compete for already over-allocated resources.

While our understanding of the atmospheric processes associated with ARs in the southwestern U.S. has progressed, many lingering questions remain on the hydrologic impacts of ARs in semi-arid regions and their role in replenishing natural and man-made reservoirs, maintaining natural ecosystem health, flooding, and droughts alleviation. Hughes et al., (2014) and Neiman et al., (2013) examined one set of AR events in January 2010 in detail, including impacts to snow accumulation, discharge, and the relationship between AR orientation and modeled precipitation. Rivera et al., (2014) looked at events across a longer record for the Verde River basin specifically, and while they primarily focused on atmospheric circulation associated with the ARs, they also briefly examined the contributions of AR precipitation to total cool season precipitation, SWE accumulations, and impacts on flood discharges. In this study, we extend the brief hydrologic analysis presented in Rivera et al., (2014) and Neiman et al., (2013) by investigating the contribution of ARs to total and intense precipitation, to changes in soil moisture, snow coverage, precipitation phase, and to extreme flooding during a 30-year period. The goals of this study are to: 1) assess the contribution of AR events to SVRB total and intense cold season (October-March) precipitation for the period 1979-2009; 2) evaluate the effect of AR impinging angle on precipitation; 3) evaluate the impacts of AR events on the basins snow cover and soil moisture conditions; and 4) investigate the link between ARs and observed extreme streamflows.

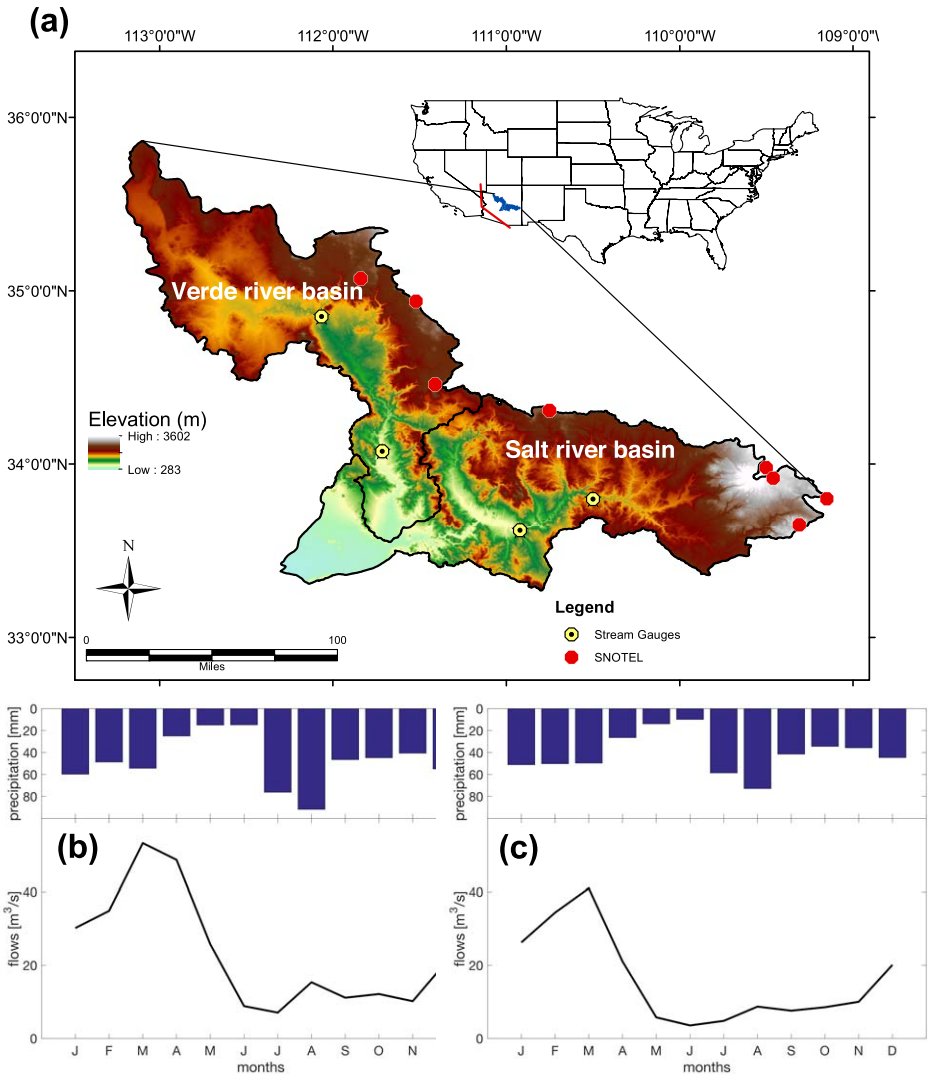

Figure 1. (a) Geographical location of the study area with the location of USGS stream gauges and SNOTEL sites. Salt river basin is located in the lower right and Verde river basin is located in the top left part of the study area. The red line shows the location of the transect used to identify the ARs reaching the basins. (top) Precipitation and (bottom) streamflow (bottom) climatology for the period 1950–2014 for (b) Salt river basin, and (c) Verde river basin.

2. Data and Methods

2.1. Observed Hydrologic Variables and Gridded Data sets

Gridded daily precipitation, minimum and maximum temperature, snow water equivalent (SWE), and soil moisture information was obtained from the data set developed by Livneh et al. (2013) (hereafter Livneh), which provides data at a 1/16° resolution for the conterminous United States for the period 1915–2011. This data set, which is an update of the Maurer et al. (2002) data set, uses observed precipitation and temperature fields from the National Climatic Data Center (NCDC) and Cooperative Observer (COOP) stations. Both variables are regridded using a synergraphic mapping system (SYMAP) algorithm as described in (Maurer et al., 2002). Hydrologic states and fluxes are simulated with the Variable Infiltration Capacity (VIC) model. Observed SWE data from nine sites in the SVRB located above 2,100 m elevation were obtained from the Snow Telemetry (SNOTEL) network (http://www.wcc.nrcs.usda.gov/snow/) starting in 1980. Additionally, daily precipitation, maximum, minimum, and mean temperature from the PRISM data set (Daly et al., 1994) were obtained for grids colocated to each SNOTEL site. Daily streamflow information was obtained from four stream gauges, two in each basin. These gauges were selected from the USGS Geospatial Attributes of

Table 1
Location of SNOTEL Sites and USGS Stream Gauges Used in the Study

	ID	Name	Lat	Lon	Elev (m)	Area (km^2)	Basin
USGS	9498500	Salt river near Roosevelt	33.62	−110.92	663.5	11,152.5	Salt river
	9497500	Salt river near Chrysolite	33.80	−110.50	1,022.3	7,378.9	Salt river
	9508500	Verde river above Horseshoe Dam	34.07	−111.72	618.4	15,172.2	Verde river
	9504000	Verde river bear Clarkdale	34.85	−112.07	952.2	9,072.7	Verde river
SNOTEL	310	Baldy	33.98	−109.50	2,781.3		Salt river
	416	Coronado Trail	33.80	−109.15	2,560.3		Salt river
	511	Hannagan Meadow	33.65	−109.31	2,749.3		Salt river
	519	Heber	34.31	−110.75	2,328.7		Salt river
	617	Maverick Fork	33.92	−109.46	2,804.2		Salt river
	861	White Horse	35.14	−112.15	2,188.5		Verde river
	488	Fry	35.07	−111.84	2,194.6		Verde river
	640	Mormon Mountain	34.94	−111.52	2,286.0		Verde river
	308	Baker Butte	34.46	−111.41	2,225.0		Verde river

Gages for Evaluating Streamflow (GAGES II) data set for their near-natural conditions—i.e., basins with no impoundments, flow diversions, or other factors that could influence natural streamflow (Falcone et al., 2010). Table 1 shows the locations of the point observations used in the study.

2.2. AR Detection

AR events are identified following the algorithm developed by Lavers et al. (2012; 2013) using vertically integrated vapor transport (IVT). We calculate the IVT magnitudes using zonal and meridional vapor fluxes from the NASA Modern-Era Retrospective Analysis for Research and Application (MERRA) reanalysis using equation (1).

$$IVT = \sqrt{QU^2 + QV^2}, \tag{1}$$

where QU and QV in kg/(m s) are the vertically integrated eastward and northward vapor flux from surface to the model top level (0.01 hPa), with 1 h temporal resolution and 1/2° × 2/3° spatial resolution.

For the years 1979–2009, we identified the time steps when the AR feature (i.e., IVT $\geq$ 250 kg m^{-1} s^{-1}) has its leading-edge impinging on the SVRB (red line in Figure 1a) and spans more than 1,500 km for the October–March period. Rutz et al. (2014) concluded that changes in the length criterion between 1,500 and 2,500 km did not affect the observed patterns and magnitude of AR frequency. The value of the IVT threshold was chosen following Rutz et al. (2014), however to evaluate how its magnitude impacted AR identification and properties, a 200 kg m^{-1} s^{-1} is also used. Second, to define the occurrence as an AR event, we required that the AR features last more than 12 h (i.e., 12 consecutive AR steps). Moreover, each AR event is defined as being at least 24 h apart from previous or subsequent events. Because each AR event might last more than 1 day, the number of days on which AR events occur could exceed the total number of AR events. In the following analysis, "AR days" refers to days during which an AR is present.

2.3. Methods

The impact of each AR event on rainfall, SWE, soil moisture, and streamflow response was evaluated for each basin. Water years (WY) were used throughout the study (i.e., the 1979–1980 winter season was assigned to the year 1980). For each winter WY, defined as October through March, the contributions of AR-related daily precipitation to *average* rainfall (exceeding the median), *heavy* rainfall (exceeding the 90th percentile), *very heavy* rainfall (exceeding the 95th percentile), and *extreme* rainfall (exceeding the 98th percentile) were estimated. A Chi-square test on equality of proportions was used to evaluate the statistical significance of the difference between AR and non-AR-related rainfall exceeding each percentile. The contribution of AR events to total seasonal precipitation was calculated as the precipitation accumulation for the day of the event (or a multiday period when the AR occurs during several consecutive days). We computed spatially distributed changes in SWE and soil moisture fields using data from the day before the onset of an AR event and 2 days after its demise to account for delayed snowmelt responses from the snowpack. To

Table 2
Sensitivity of AR Detection to Threshold Choice

		Salt river basin		Verde river basin	
IVT	kg/(m s)	200	250	200	250
Number AR events		218	122	218	122
Mean (Max) number per year		7.2 (13)	4 (9)	7.2 (13)	4 (9)
Mean (Max) duration	days	2.4 (9)	2.2 (8)	2.4 (9)	2.2 (8)
Mean (Max) event precipitation	mm	16.5 (173)	18.9 (163)	17.1 (178)	20.3 (165)
Mean (Max) year precipitation	mm	120.4 (429)	124.4 (441)	77.1 (356)	82.5 (376)
Mean (Max) AR precipitation to seasonal total	%	39 (70)	44 (58)	25 (72)	29 (61)

Note. Maximum values are indicated within brackets.

account for the uncertainty of the gridded rainfall and temperatures used in the analysis, we compared the Livneh to the high spatial resolution (~ 800 m) PRISM data set (Daly et al., 1994).

To explore the relationship between AR and flooding on the SVRB, the largest observed flow for each year (during the cold season) was selected from each of the four stream gauges to create an Annual Maximum Series (AMS) of maximum flows. A Log-Pearson III distribution function (USGS, 1982) was fit to the data to evaluate the probability of exceedance of AR-related flows. The Maximum Likelihood method was used to fit the theoretical distribution to the observations; the goodness of the fit was evaluated with the Anderson-Darling (A-D) and Kolmogorov-Smirnov (K-S) nonparametric tests. Runoff coefficients (RC), a dimensionless coefficient defined as the ratio between specific flows (streamflows divided by the contributing area in millimeters) and the mean areal precipitation, were computed for each gauging station for all days with and without the occurrence of an AR. Following the approach of (Guan et al., 2016), the RCs for AR events were computed from the day prior to the onset of the event and the day after its demise in order to include delayed basin responses. To assess the impact of the warmer temperatures, associated with the AR events on the generation of runoff in the basins, the differences in the contributing areas under AR and non-AR conditions were calculated. The contributing area is defined as the percentage of the basin above the melting line (elevations where the mean daily temperature is less or equal to 0°C).

3. Results

3.1. Climatology of ARs in the SVRB

An IVT threshold equal to 250 kg/(m s) was used to identify ARs in the SVRB following Rutz et al. (2014) who indicated that the spatial pattern of AR occurrences across the entire Western U.S. did not change

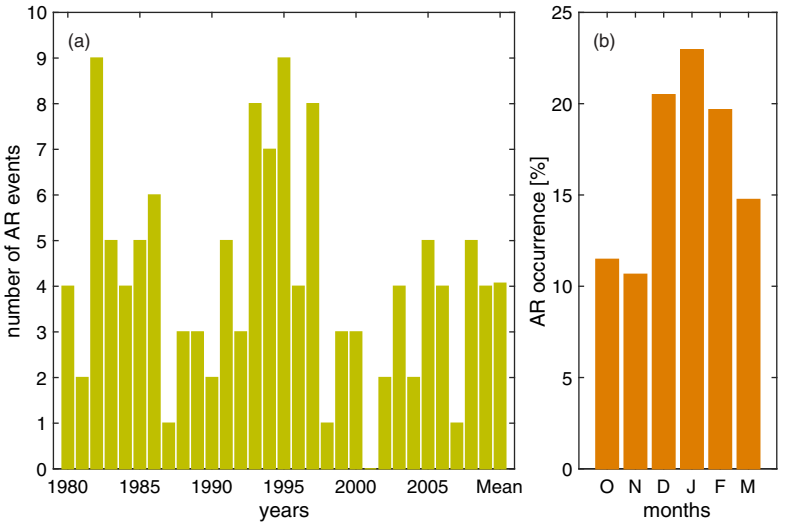

Figure 2. (a) Frequency of AR event occurrence per year for the period water year (WY) 1980–2009. The multiyear mean is shown in the rightmost bar. (b) Seasonal frequency as percentage of days with observed events as a function of months.

with different thresholds. However, since these authors also indicate that the frequency of ARs changes with the IVT threshold, we evaluated the sensitivity of AR identification when a lower (200 kg/(m s)) threshold is used. Table 2 shows that the lower threshold allows for the identification of a larger number of ARs (218) compared to the higher threshold (122), which constitutes a 78% increase in the number of events. On average for the 30 year period, the mean number of AR events increases from 4 to 7.2 events per year for the 250 and 200 (kg/(m s)) thresholds, respectively (supporting information Figure S1). Since our interest is in evaluating extreme events, and to make our results comparable to previous studies in the Western U.S., we adopted the larger IVT threshold for our analysis. A total of 122 AR events were identified over the SVRB during the cold seasons of 1979–2009 (supporting information Table S1). While this total equals an average of four events per year for the period, there was large interannual variability in the number of events. The largest number of events occurred in WYs 1982 and 1995 (nine events each year) and WYs 1993 and 1997 (eight events each year). No events were observed during WY 2000 and only one event was identified in WYs 1987, 1998, and 2007 (Figure 2a). During the cold season, AR events are more frequent in the middle of the winter (December–February); 60% of them occur during this period (Figure 2b), with a January maximum. These results are consistent with the seasonality found by Rutz et al. (2014).

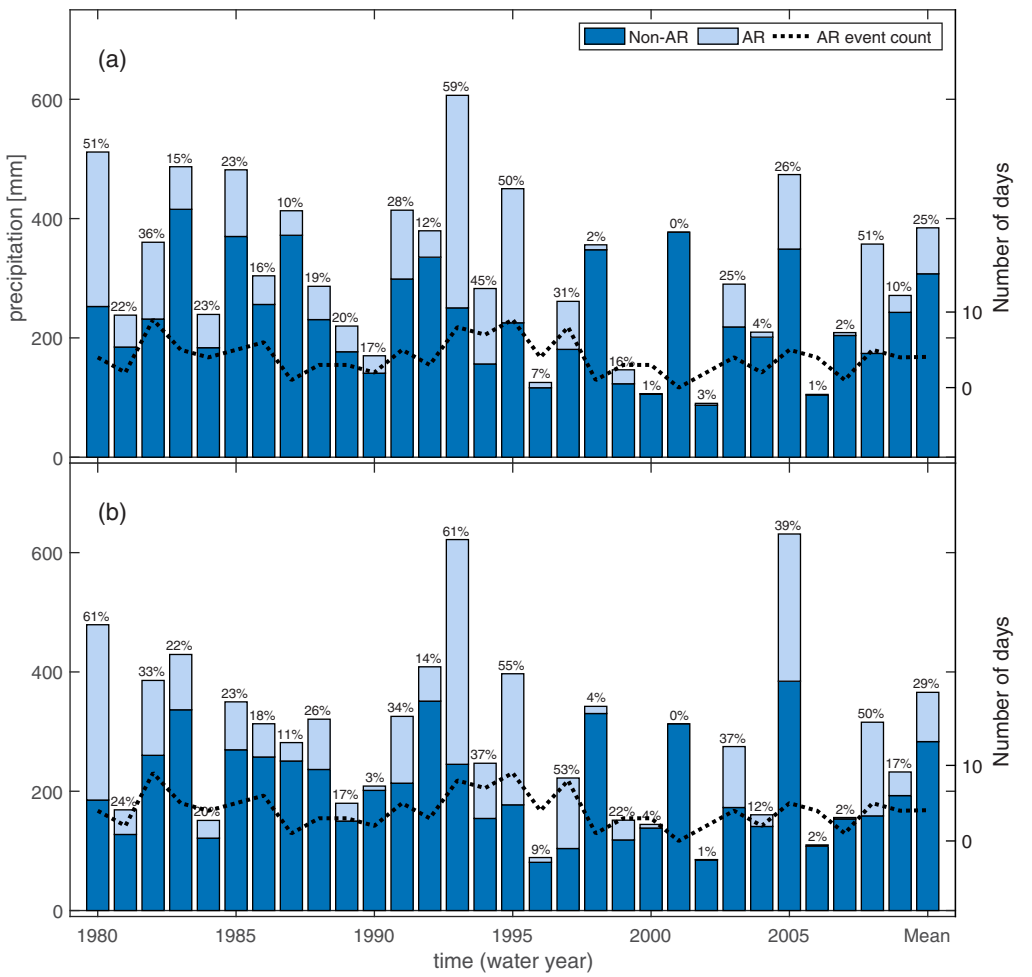

Figure 3. Seasonal observed precipitation (October–March) over the (a) Salt and (b) Verde river basins. Total precipitation for each year is shown in each bar (light blue and dark blue) and the AR contribution to total seasonal precipitation is indicated in light blue. The percentage contribution of ARs to total seasonal precipitation is shown with the numbers on top of each bar. The number of AR events per year is indicated by the dotted line in the top plot. Period water years 1980–2009. The multiyear mean is shown in the rightmost bar.

3.2. Precipitation, SWE, and Temperature During AR Events

The AR contribution to total seasonal precipitation varies greatly throughout the 30 years analyzed, ranging from 0% to approximately 60%. The average contribution for the study period was 25/29% of the total seasonal precipitation (Figure 3). Note that the average contribution for the lower (200 kg/(m s)) threshold was 39%/44% and the maximum 70%/72% for the Salt/Verde river basin, respectively. Despite the differences, the Wilcoxon test (5% significance level) indicates no statistically significant differences in the medians of AR event precipitation for the lower and higher threshold (Figures S2 and S3 Supporting Information). The 1993 WY was exceptional not only for the largest total seasonal precipitation, but also for the largest AR-related precipitation, with 59%/61% for the Salt/Verde river basins, respectively. The extreme precipitation of 1993 resulted from an anomalous circulation pattern, which consisted of an unusually high number of alternating warm and cold storms in most of Arizona (House & Hirschboeck, 1997). One of the features that differentiated the WY 1993 event from the 1982 event, which had nine ARs (Figure 2a), was the high frequency of ARs during a little over a month period: the WY 1993 had six AR events with durations ranging from 2 to 3 days whereas the WY1982 event had only three ARs with durations no longer than 2 days. During a 3 month period, excess precipitation and increased snowmelting contributed to the development of flood-enhancing antecedent soil moisture conditions in the region, eventually resulting in losses of life and heavy impacts on the local economy. To evaluate the uncertainty in the gridded precipitation and temperature values used in our analysis, we compare at each SNOTEL site daily, seasonal, and annual precipitation, maximum, minimum, and mean temperature with the PRISM data set. The comparison indicates that the Livneh data set has systematically higher precipitation estimates than PRISM at the three aggregation levels (supporting information Figures S4 and S5). Temperatures in both data sets are highly correlated with correlation coefficients ranging from 0.79 to 0.96; however, the Livneh temperatures are cooler than PRISM values for all three variables (supporting information Figures S5 and S6).

Clearly, ARs have a significant impact on the total precipitation during the cold season (Figure 3). Since our interest is also to evaluate their contribution to hydrologic extremes, for each basin we computed the contribution of ARs to daily precipitation exceeding the 50th (*median* rainfall), 90th (*heavy* rainfall), 95th (*very heavy* rainfall), and 98th (*extreme* rainfall) percentiles. For each percentile, first we added the daily exceeding rainfall for days with AR events; then we estimated the AR contribution as a percentage of the observed cumulative rainfall above the threshold during the study period (Figure 4). ARs contributed to 26%/30% of the total seasonal precipitation over the median for the Salt/Verde river basins. However, the assessment of more intense events (those exceeding the 90th 95th, and 98th percentiles) showed that the percentage of the total seasonal rainfall attributable to AR events increased to 40%/44% for rainfall above the 90th percentile and to 52%/55% and 64%/72% for *heavy* and *very heavy* rainfall, respectively. To evaluate if the AR

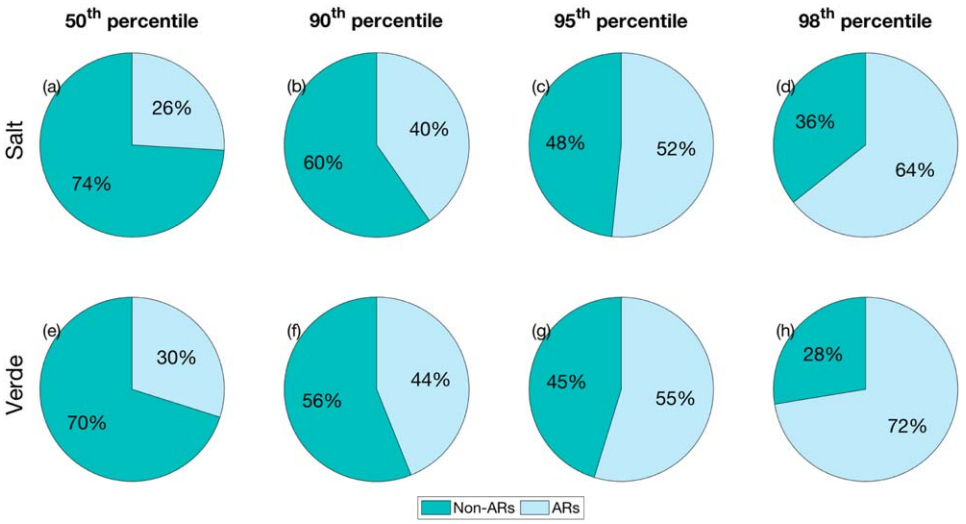

Figure 4. Contribution of AR events to median (>50th percentile), heavy (>90th percentile), very heavy (>95th percentile), and extreme (>98th percentile) rainfall. Basin-averaged precipitation for the period 1980–2009. Salt river basin in the top and Verde river basin in the bottom plot, respectively.

Table 3
Chi-Square Test for Equality of Proportions Between AR and Non-AR Rainfall Exceeding a Set Threshold: Median (>50th Percentile), Heavy (>90th Percentile), Very Heavy (>95th Percentile), and Extreme (>98th Percentile) Rainfall

	50th percentile		90th percentile		95th percentile		98th percentile	
	Non-AR (AR)	χ^2	Non-AR (AR)	χ^2	Non-AR (AR)	χ^2	Non-AR (AR)	χ^2
Salt river basin	0.700 (0.252)	0.523	0.352 (0.039)	1.525	0.248 (0.016)	**5.65**	0.130 (0.005)	**22.49**
Verde river basin	0.789 (0.253)	1.15	0.393 (0.039)	0.817	0.270 (0.015)	**4.42**	0.156 (0.004)	**16.58**

Note. Basin-averaged precipitation for the period WY 1980–2009 for the Salt and Verde river basins. The critical χ^2 value for alpha 0.05 and one degree of freedom is 3.84. Bold values indicate statistically different proportions based on a sample size of 270/5190 for the AR/non-AR cases, respectively.

contribution to total precipitation was statistically significant, we performed a Chi-square test for equality of proportions between AR and non-AR for the different categories of precipitation. The proportions test was chosen to consider the different sample sizes: 270 AR days and 5,190 non-AR days during the 30 year period. The Null hypothesis of equality of proportions was tested at the 5% significance level. Table 3 shows that the proportion of AR *medium* and *heavy* rainfall equals the proportion during Non-AR events therefore there is no evidence to reject the null hypothesis. For daily rainfall exceeding the *very heavy* and *extreme* thresholds, the calculated χ^2 is larger than the critical value therefore there is enough evidence to reject the Null hypotheses and declare a significant difference between AR and non-AR rainfall. This indicates that despite the relatively low frequency of AR occurrences in the SVRB, their contribution to seasonal extreme precipitation is significant for the region.

Table 4 shows the number of AR days with precipitation above the thresholds as percentage of the total number of AR days (270). It can be seen that 10.4%/4.1% of the days with an AR event have no rainfall indicating that there is not always causality between the two variables. The number of AR days with *heavy* rainfall represents 35.2%/39.2% of the total, while the number of days with *extreme* rainfall represent 13.0%/15.6% for the Salt/Verde river basins. These results indicate the AR-related rainfall is not only vital for sustaining water services in the basins, but also can be related to hydrologic extremes (as we will evaluate in section 4).

As is the case on the Pacific coast, the strength of the AR in inland Arizona, its width, and wind orientation relative to the mountains dictates the amount of precipitation (Ralph et al., 2013). Figures 5a and 5b show that ARs mean precipitation and mean IVT are linearly correlated with statistically significant ($p < 0.05$) coefficients of 0.52 (Salt river) and 0.59 (Verde river). The mean IVT for AR events ranges from 270 to 574 kg/(m s) with a mean value of 380 kg/(m s) whereas the mean precipitation ranges from 10 to 39.4 (42.2) mm, after applying the 10 mm threshold. In general, large precipitation events are linked to large daily maximum flows (denoted by the size of the circle). Larger flows tend to occur with large IVT (larger than ~350 kg/(m s)) and when mean precipitation exceeds 15 mm/d, however the relationship between streamflow magnitude and IVT is not clear. For instance, in Figure 5a an IVT value of 500 kg/(m s) can be associated a to medium (~100 m^3/s) or to a large (~500 m^3/s) streamflow value corroborating the nonlinear response of the basins.

Table 4
AR Days With Rainfall Above a Certain Percentile Indicated in the Threshold Column as a Percentage of the Total Number of AR Days (270)

		Number of days exceeding threshold (%)	
Precipitation	Threshold (mm) Salt/Verde	Salt	Verde
No rain (zero rainfall)		10.4	4.1
Heavy rainfall (> 90th)	8.6/8.2	35.2	39.3
Very Heavy rainfall (> 95th)	13.4/13.0	24.8	27.0
Extreme rainfall (> 98th)	19.8/20.1	13.0	15.6

Note. Results are based on 122 AR events identified during the 1980–2008 period. Daily rainfall values are averages for each basin.

We evaluate the impact of AR impingent angle, i.e., angle with respect to the mountain range, on mean event precipitation and mean IVT by binning the angles into three categories: meridional angles (0°–40°), orthogonal angles (40°–50°), and zonal angles (50°–90°), with the 0° located north. Our results were not found to be sensitive to changes in the width of the orthogonal bin (not shown). In the Salt river basin, where the mountain range is more east-west oriented, mean precipitation and mean IVT are statistically correlated ($p < 0.05$) for meridional ($r = 0.54$) and orthogonal ($r = 0.84$) impinging angles. Conversely, for zonal angles, i.e., fluxes almost parallel to the mountain range, the correlation between precipitation and IVT is almost zero. In the Verde river basin, where the mountain range is northeast-southwest oriented, zonal, and meridional impinging angles have a similar efficiency to convert IVT to precipitation (Figure 5d).

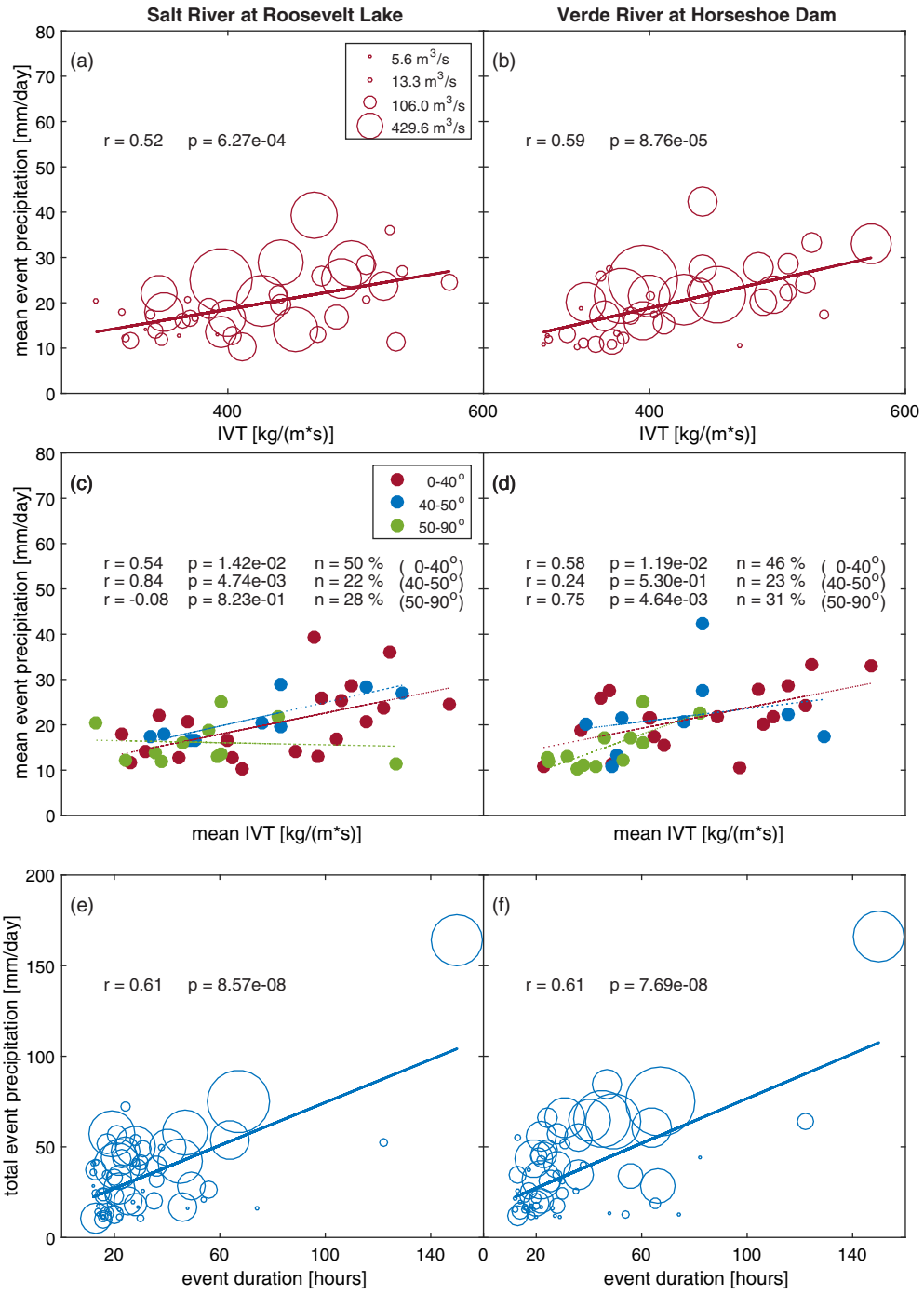

Figure 5. (a) and (b) AR event mean precipitation as a function of mean vertically integrated vapor transport (IVT); (c) and (d) idem as (a) and (b) but for different impinging angles; (e) and (f) and total event precipitation as a function of event. The size of the circle denotes the magnitude of maximum observed flow for each AR event. Correlation coefficients (r), *p* value (*p*), and number of AR events as percentage of the total (n).

The average duration of the AR events is 21 h, with a range of 12–150 h. There is a positive correlation ($p < 0.05$) between the duration of the AR event and the event total precipitation, with correlation coefficients (r) of 0.61 for both basins (Figures 5e and 5f), however, maximum flows are not strongly related to event duration. These results indicate that neither IVT nor event duration are directly related to runoff generation in the basins, because many AR events have high-IVT and duration yet low maximum daily flows.

This suggests that during AR events precipitation can fall as snow or as liquid, which freezes into the snowpack, and thus does not always trigger extreme runoff conditions. The connection between ARs and runoff processes is addressed in section 4.

Figure 6 shows the contribution of AR events to basin-averaged SWE in the basins. For each WY, first we compute mean daily SWE for the SNOTEL sites located in each basin (Table 1) and second, we select the maximum SWE value for each season. Then, following Guan et al. (2016), the deltas in basin-average SWE between the day after the demise and the day prior to the onset of an AR event are computed. When the delta is positive, on average, there is snow accumulation at the SNOTEL sites; when the delta is negative rain-on-snow or snowmelting occur. For both basins during the period studied, ARs have consistently contributed to more snow accumulation than to decreases in the snow pack. Note that the deltas, either positive or negative, represent the sum of the changes for each AR event. During the 30 year period, 15 ARs are related to negative changes in SWE in both basins, 65/69 events are linked to positive changes in the Salt/Verde river basins, and 42/48 events are not linked with changes in snow cover for the Salt/Verde river basins. The WY 1985 has the largest AR-related negative SWE deltas, whereas the largest AR-related SWE accumulation in the basins occurred during WY 1993. That year, approximately 60% of the total seasonal precipitation is linked to AR occurrences (Figure 3). It is worth noticing that these deltas are averaged for the different topographic elevations in the basins, so the variation of positive/negative changes at different elevations is not represented in our analysis. Furthermore, the Verde river basin does not have SNOTEL sites above 2,286 m elevation while every site in the Salt river basin is located above that elevation, which may have introduced biases in the analysis.

In California's Sierra Nevada Mountains, AR occurrences during the 1998–2014 period accounted for 50% of the rain-on-snow events, due to above-freezing temperatures. These rain-on-snow events lead to enhanced runoff due to rainfall and snowmelt in the region (Guan et al., 2016). For the SVRB, we analyzed observed SWE values from nine SNOTEL sites to evaluate the contribution of ARs to rainfall and snowmelting in the basins. For each site, daily precipitation and maximum and minimum temperatures from the Livneh data set are obtained for the closest grid cell. Figure 7a shows SWE deltas as a function of mean daily temperature for all sites and for all days with and without AR occurrences. The magnitude of the circle indicates total

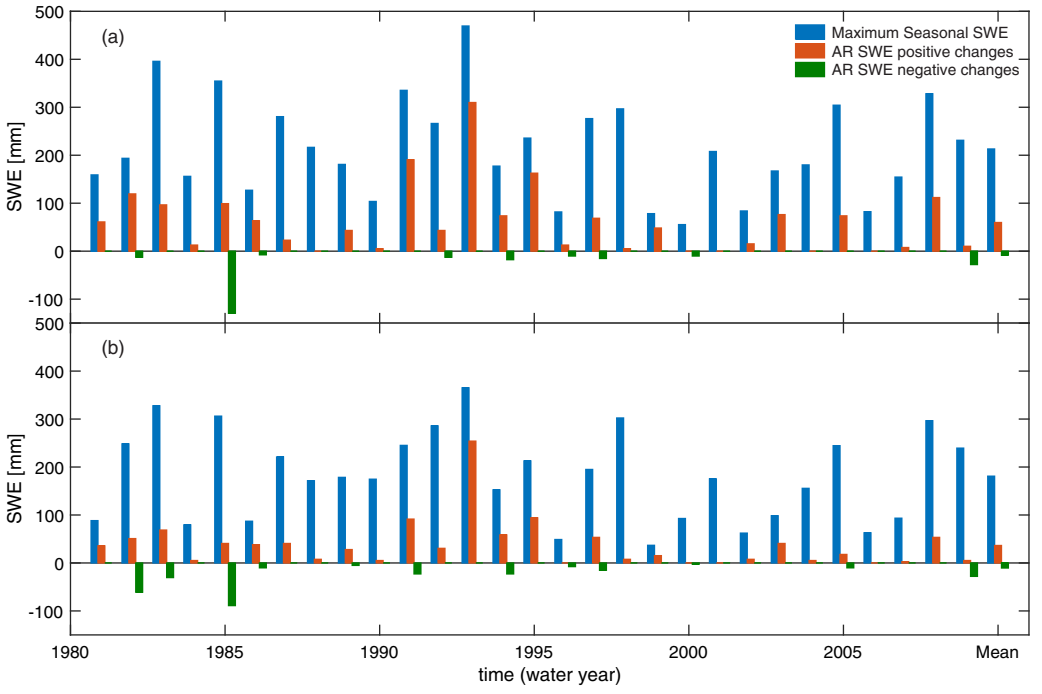

Figure 6. Climatology of SWE for the (a) Salt and (b) Verde river basins. The blue bars show the maximum basin-averaged SWE accumulation for each season from nine SNOTEL sites. The green/orange bars denoted the sum of all positive/negative changes in SWE during AR events.

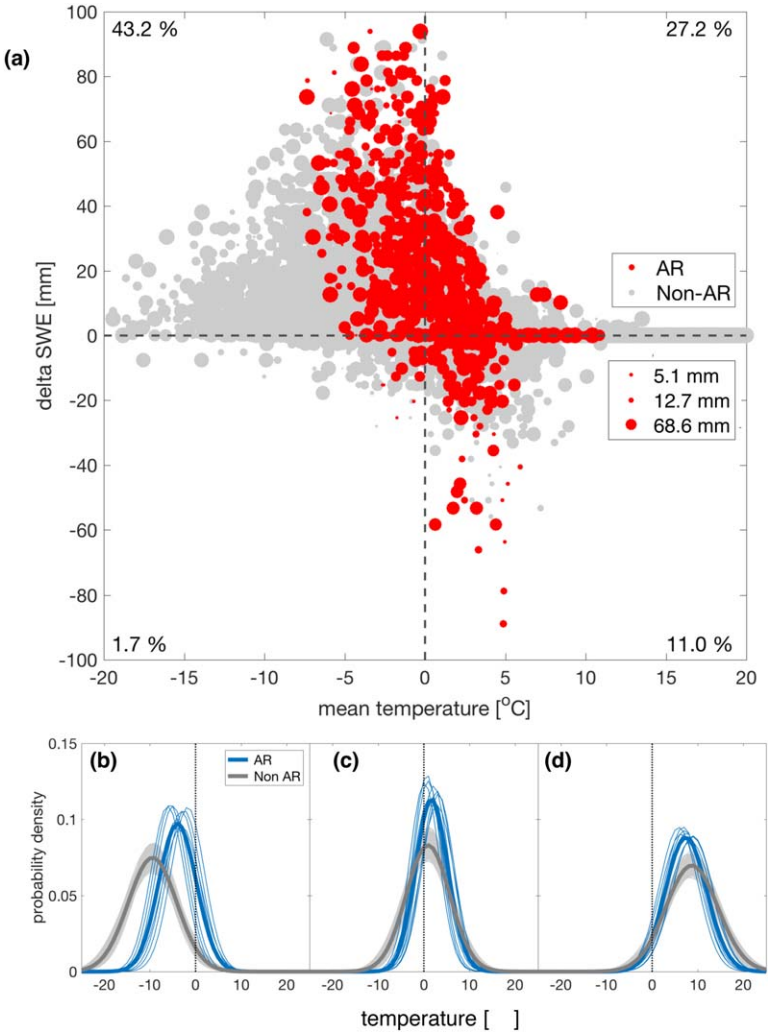

Figure 7. Changes in SWE as a function of mean (a) temperature during AR events (red circles) and non-AR events (gray circles) at nine SNOTEL sites. The size of the circle is proportional to the total daily precipitation. Note that only days with precipitation exceeding the 5 mm/d threshold are shown. The percentages indicate the number of AR events (with respect to the total of AR events) for each delta SWE-temperature combination average of across the nine sites. (bottom) Probability distribution of (b) minimum, (c) mean, and (d) maximum temperatures at a collocated grid cell.

daily precipitation (exceeding 5 mm/d for individual days and for event averages). The majority of days with precipitation have mean temperatures below freezing, a situation that contributes to snow accumulation in the basins (positive delta SWE). During AR events at the nine SNOTEL sites, 43.2% of the events occur in below-freezing conditions that lead to snow accumulation in the basins. As expected, the number of cases with positive SWE deltas increases with topographic elevation from ~25% at 2,200 m altitude to ~67% at 2,800 m (supporting information Figure S7a). On the other hand, 27.2% (8%–48% range) of the AR events occur with above-freezing conditions but still exhibit positive changes in SWE (snow accumulation), suggesting that liquid water falling on snow might be absorbed in the snowpack and consequently measured by the SNOTEL snow pillow as an increase in SWE or the presence of snow. The presence of rain, snow, or mixture of the two has been observed for temperatures in between 0° and 3° in the Sierra Nevada in California (Lundquist et al., 2008; Figure 10c). These authors indicate that at 1.5° the percentage of snow occurrence is 50%, and on average, 50% of measured precipitation contributes to increases in snowpack. We speculate that at low elevations, where more incidents with increases in SWE and above-freezing temperatures are found (supporting information Figure S7b), the rain-on-snow processes are more likely to occur and are thus measured as SWE by SNOTEL snow pillows. These processes will be less frequent at higher elevations.

Positive increases in SWE were reported by Neiman et al. (2013) for one AR event that impinged on Arizona in 2010. We also found that 11% of the days with ARs register above-freezing temperatures and a negative delta SWE, pointing to rain-on-snow processes or snowmelting.

Observed minimum, mean, and maximum daily temperatures from the Livneh grid cells at the colocated SNOTEL sites are fitted with a normal distribution (Figures 7b–7d). To account for the difference in sample sizes, from the time series of daily temperature we randomly select 1,000 sampling of 252 (the number of AR days with precipitation above 5 mm) non-AR temperature values and fit the probability distribution to each sample. During the occurrence of ARs, minimum daily temperatures are significantly warmer than during non-AR events, as a result of the strong warm air advection that accompanies AR landfalls. Differences in minimum temperature are statistically significant at the nine sites as measured with the Student *t* test (5% significance level). Differences in AR and non-AR maximum temperatures are found to be statistically different for the five sites in the Salt river basin, and mean temperatures are found to be statistically different in three out of five sites in the Salt river basin and in the four sites located in the Verde River basin. It is worth noticing that the daily mean temperature is computed as the arithmetic average between the minimum and maximum temperature, and it might not represent the actual observed mean value. The results indicate that air temperatures are warmer during AR events and can result in snowmelting and/or rain-on-snow processes in the basins and potentially contribute to extreme flooding events.

The location of the snow melting line has important implications for the generation of runoff in snow-dominated basins (Lundquist et al., 2008). We analyzed whether the warmer than normal temperatures during AR events (as shown in Figure 7) resulted in additional runoff as the melting line rose and the basins' contributing areas increased. In the SVRB the melting line (defined as elevations with 0°C mean daily temperature) is located between 1,500 and 2,100 m or even as high as 2,400 m (White Mountain Apache Tribe, personal communication, 2016). Figure 8a illustrates that mean daily temperatures for the WY 1980–2009 are on average warmer during AR events in the Salt river basin, but not in the Verde river basin. This raises

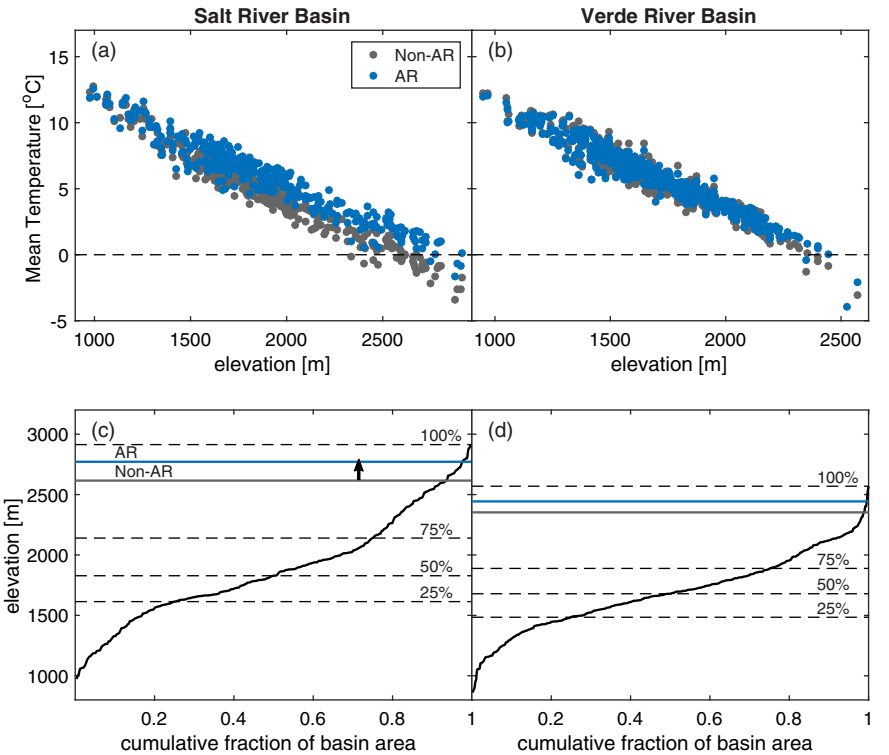

Figure 8. Mean daily temperatures for different topographic elevations in the (a) Salt and (b) Verde river basins for AR and non-AR events. Cumulative fraction of the basin contributing to surface runoff as a function of topographic elevations in meters for (c) Salt river basin and (d) Verde river basin. The horizontal-dashed lines show the percentage of the basin below a certain elevation. Solid lines show the melting level, defined as the elevation with a mean daily temperature of 0°C for the water years 1980–2009, during AR events (blue) and non-AR conditions (gray).

the location of the melting line to higher elevations, especially in the Salt river basin, which has taller peaks than the Verde river basin. During non-AR conditions, 75% of the basin contributing to runoff generation is below 2,140/1,880 m in the Salt/Verde river basins, respectively (Figure 8c and 8d). Warmer than normal temperatures during AR landfallings raise the melting line from 2,615/2,352 m to 2,771/2,443 m and increase the contributing area on average from 77%/83% under non-AR conditions to 91%/93% under AR conditions for the Salt/Verde river basins, respectively. Neiman et al. (2013) in their analysis of the intense AR event in the SVRB that occurred on 21–22 January 2010, found that 90%–98% of the Salt river basin received rainfall rather than snow. These results suggest that precipitation during AR events is more likely to be liquid over large areas of the basin, which increases soil moisture conditions and enhances runoff generation.

Since streamflow generation is influenced by soil moisture conditions in the basins, we computed composites of spatially distributed total precipitation and deltas in SWE and soil moisture from the Livneh data set for all the AR events with total precipitation exceeding 5 mm. The soil moisture values used in the analysis are VIC model simulated state variables and therefore prone to high uncertainty. In the SVRB the lack of soil moisture observations did not make possible a model validation, however Livneh and Hoerling (2016) showed that there is a good agreement at the monthly time step between VIC simulations and GRACE estimates, and the Unified Land Model (ULM) model which gives us confidence in our results. The correlation coefficient between SNOTEL observations and VIC-simulated maximum SWE at each site ranged from 0.74 to 0.93, indicating that the VIC model can realistically represent snow processes in the basins (supporting information Figure S8). Based on the composite of all AR events, daily total precipitation on average ranges from 10 mm at lower basin elevations to up to 60 mm in the basins' headwaters (Figure 9a). The increase in

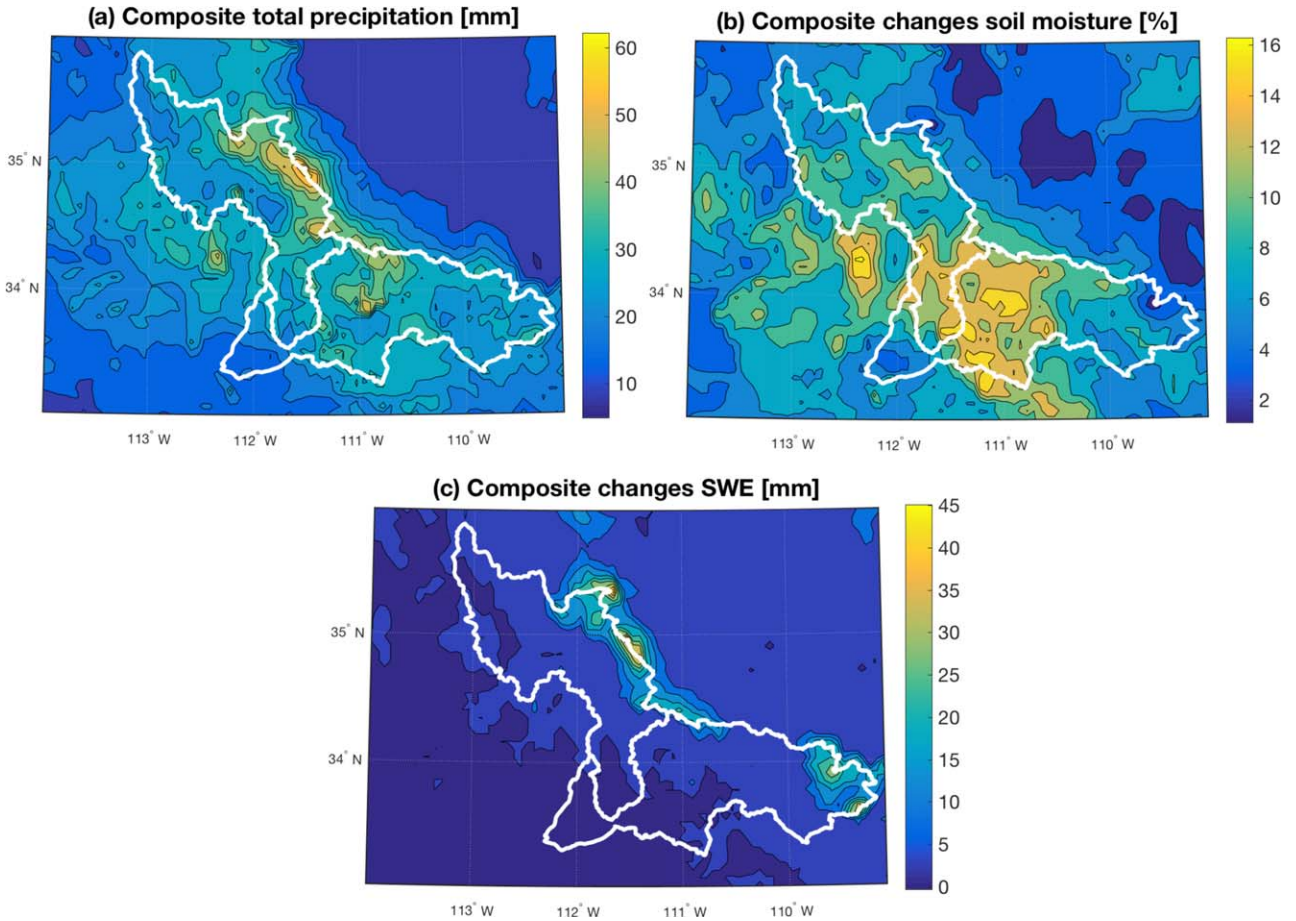

Figure 9. Composite of (a) mean total precipitation during AR events, (b) changes in soil moisture, and (c) changes in SWE. Changes are computed for each grid cell as the difference between the day prior to the AR onset and the day after its demise. Period 1980–2009. The white line shows basin boundaries.

soil moisture between the day prior to the AR onset and the day following the AR demise ranges from 2% to 16% (Figure 9b). The largest changes are found in downstream areas, not in higher elevations where most precipitation takes place. The lack of changes in soil moisture at higher elevations is due to frozen soils under the snowpack during the winter months. Composite changes in SWE are positive mostly at the higher elevations directly above the melting line (Figure 9c).

4. Streamflow Characteristics During AR Events

This section evaluates the surface responses of the SVRB to AR events. We began by computing the RCs for any given day—i.e., days with and without AR events—for precipitation exceeding a 5 mm threshold. We excluded small precipitation totals to filter out anomalously larger RC values resulting from a small number in the denominator. Larger RCs indicate areas with low infiltration and high runoff, and therefore represent the flashiness of a basin during storms as overland flow moves faster to the main channel. Figure 10 shows that the 25th, 50th, 75th, and 90th percentiles of all computed RCs for the four stream gauges are consistently larger during AR events than during non-AR events. Note that in the Verde river basin a larger drainage area and smaller flows (Figure 1c) generate smaller RCs compared to the Salt river basin, despite similar total seasonal precipitation amounts in both basins. For those days with ARs, on average, RCs are 46.8%, 36.5%, 8.9%, and 20.8% larger than RCs during non-AR days for the four stream gauges; this indicates that additional runoff is generated in the basins by an increase in contributing areas (i.e., the rise of the melting line) or by rain-on-snow processes. Larger changes in RC occur in the Salt river basin, and these changes coincide with statistically significant differences in the medians as tested by the two-sided Wilcoxon rank

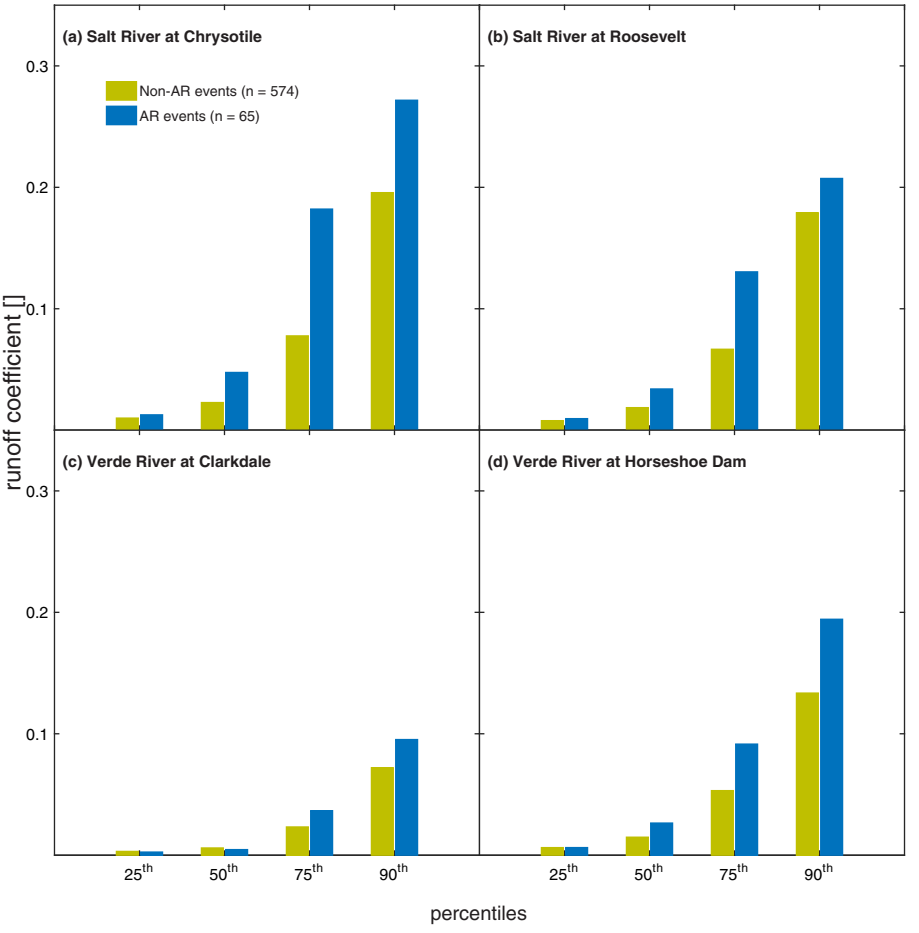

Figure 10. Percentiles of runoff coefficients composited over all days with observed precipitation (green bars) and over ARs (blue bars). (a) Salt river near Chrysotile, (b) Salt river near Roosevelt dam, (c) Verde river near Clarkdale, and (d) Verde river below Tangle Creek. Period 1980–2009.

sum test (5% significance level). The Verde river basin has smaller RC changes, and the differences in the medians from AR and non-AR events are not statistically significant. The different behavior in the Verde is likely due to lower elevations in the basin, different impingent angles of the ARs relative to the mountain range orientation, or to basin response to antecedent moisture conditions.

Flow duration curves are defined as the percentage of time that flow in a stream is likely to equal or exceed a particular value. These curves were calculated for daily winter flows for the Salt river at Chrysotile and Roosevelt and the Verde river at Horseshoe Dam from 1950 to 2014 (Figures 11a, 11b, and 11d), and for Verde river at Clarkdale from 1966 to 2014 (Figure 11c). We use the longest available records for the basins to include extreme flows that have been observed outside the analysis period. By including only days with at least 5 mm of rainfall, the number of days with an identified AR event is reduced from 270 to 178 for the Salt river basin and 205 for the Verde river basins. AR-related daily flows (green circles) are found across the whole spectrum of exceedance probabilities, not only for extreme flow conditions. However, on average ~24% (range 22%–26%) of AR-related daily streamflows exceed the 95th percentile and ~40% (range 30%–57%) exceed the 90th percentile in all four gauging stations. This supports the previous findings that ARs generally produce greater runoff, but this result also indicates that ARs also contribute to lower intensity events.

We analyzed the rarity of AR-related flows from a statistical perspective by performing a flood frequency analysis of annual maximum (AMS) daily streamflows (AR and non-AR) observed at the four stream gauges. This approach, widely used for extreme value analysis and for hydrologic design, selects for each WY the largest observed flows and utilizes a Log-Pearson III probability distribution function to describe their statistical properties. To account for the delay in the basins' response to AR occurrences, the maximum observed flow is obtained from a window spanning the duration of the AR plus the day following the end of the event. The goodness of fit of the theoretical distribution function to observations, using the Maximum Likelihood method, was evaluated for all four gauges (5% significance level) with the Anderson-Darling (A-D) and Kolmogorov-Smirnov (K-S) nonparametric tests (Figure 12). The magnitude of the observed and theoretical (Log-Pearson III) flows are plotted as a function of the return period (years) for the four stream gauges. The inset in each subplot shows the magnitude of maximum flows that are AR-related and their return period for the period 1980–2009. On average, 43% of the AMS flows were linked to AR occurrences

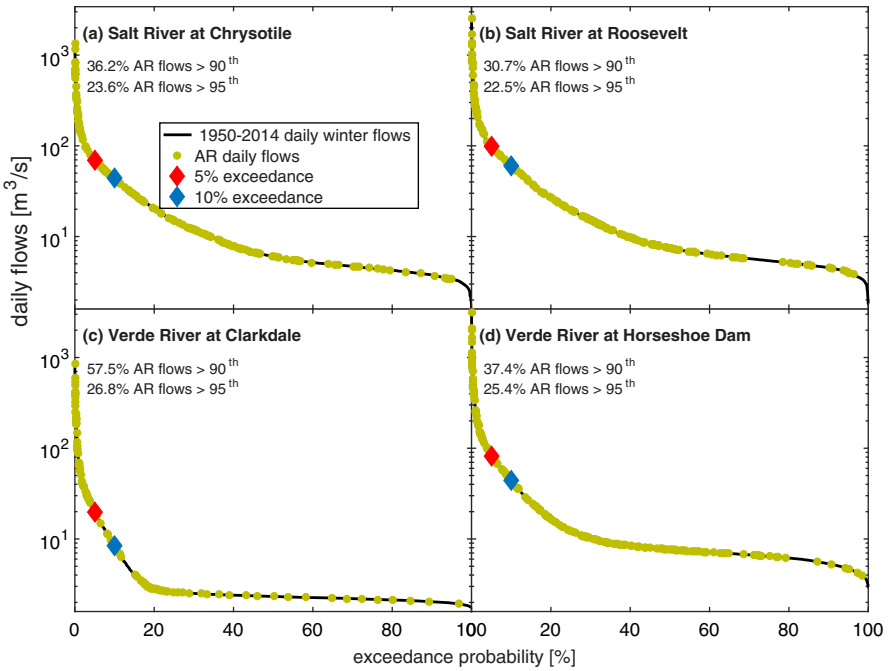

Figure 11. Flow duration curve of daily winter streamflows (October–March) for four USGS stream gauges in the basins. Period 1950–2014 except for the Verde river at Clarkdale which is 1966–2014. The black line denotes all the daily streamflow values for the period, the green circles denote AR-daily flows, and the red/blue diamonds show the observed 90th/95th percentiles, respectively.

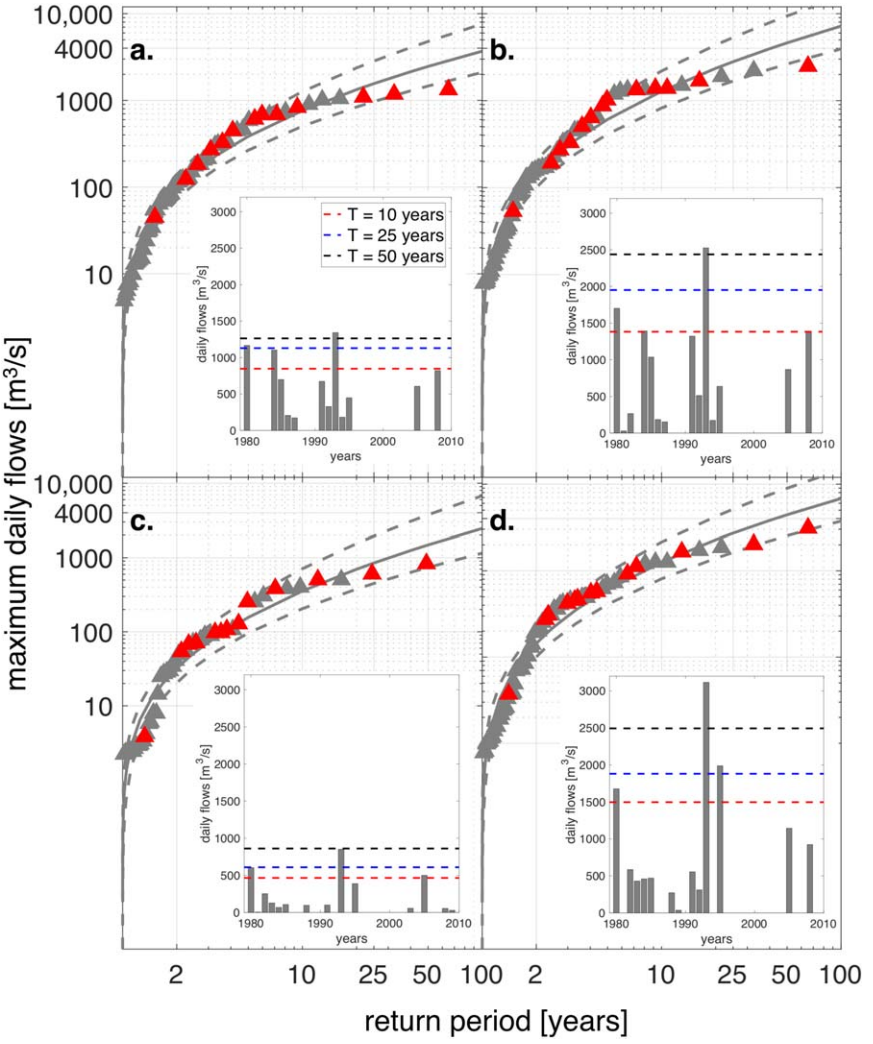

Figure 12. Annual maximum flows at each stream gauge for the period 1950–2014. The triangles denote observed values, red triangles denote AR events, the solid line is the fitted Log-Pearson III distribution, and the dashed lines the 5% and 95% confidence intervals. The inset in each subplot show the magnitude of AR-related maximum flows for the period 1980–2009 with the horizontal dashed lines depicting the 10, 25, and 50 year return periods. (a) Salt river at Chrysotile, (b) Salt river at Roosevelt, (c) Verde river at Clarkdale, and (d) Verde river at Horseshoe Dam.

in the SVRB, with 25% of the events exceeding the 10 year return period. Maximum flows for WY 1993 had a return period of 65 years, with magnitudes of 1,342 and 2,525 m^3/s for the two gauges in the Salt River basin and 849 and 3,114 m^3/s for the two gauges in the Verde river basin. To put these magnitudes into context, the mean AMS flows for the four stream gauges are: 269 m^3/s for the Salt river at Chrysolite, 449 m^3/s for the Salt river at Roosevelt, 121 m^3/s for the Verde river at Clarkdale, and 432 m^3/s for the Verde river at Horseshoe Dam. The 1993 AR-related flooding was an order of magnitude larger than the mean maximum flow observed in the basins.

5. Conclusions

Daily streamflow observations from four stream gauges in the Salt and Verde river basins in semiarid northeastern Arizona are combined with SNOTEL observations, gridded precipitation, SWE, temperature, and soil moisture to explore the role of ARs on the hydrologic surface response in the region. Using IVT estimates from MERRA reanalysis of cold season (October–March) data for the period 1979–2009, we identified 122 landfalling AR events with an average duration of 21 h. The number of identified AR events was sensitive to the IVT threshold used, with lower thresholds lending a larger number of events. An average of four AR events per

year are found for the period, with large interannual variability ranging from no events to a maximum of nine events per year (WYs 1982 and 1995) and eight events per year (WYs 1993 and 1997). ARs are found to be more frequent in December, January, and February that in the other months of the cold season, as more than 60% of the landfalling events identified occur during these months. The AR impinging angle with respect to the mountain range orientation had an impact on the efficiency to convert IVT into precipitation.

The ARs reaching semiarid northeastern Arizona have a large impact on seasonal precipitation, contributing to up to 60% of total seasonal precipitation. However, this contribution has large interannual variability. Of the daily precipitation exceeding the daily 90th percentile, on average, 42% comes from ARs, however for daily precipitation exceeding the 98th percentile, the percentage attributable to AR increases to 64%/72% for the Salt/Verde river basins. This shows that, despite ARs being relatively infrequent during the cold season, the portion of extreme events resulting from them is significant and can have significant negative and positive impacts on the region.

During AR storms, the partitioning of precipitation into rainfall and snow is conditioned by the advection of warm air typical of these events. Changes in observed SWE are mostly positive (increases) and coincide with below-freezing temperature conditions in the basins (~43% of the events). However, 27% of the events occur during above-freezing mean temperatures and result in positive changes in SWE, suggesting liquid precipitation retained on the snowpack or snow. Conversely, negative changes in SWE during above-freezing temperature indicate rain-on-snow processes, snowmelting, or an increase in the percentage of the basin generating runoff as the melting line rises. Statistically significant warmer-than-normal temperatures (at the 5% level) are found during AR occurrences due to the strong warm air advection that accompanies their landfalls. As result, the location of the melting line rises from 2,615/2,352 m to 2,771/2,443 m and the average basin contributing area increases from 77%/83% under non-AR conditions to 91%/93% under AR conditions for the Salt/Verde river basins.

Increases in soil moisture mostly in lower elevations result from increases in precipitation during AR events. Not all AR events are linked to extreme flooding in the basins; however, the 25th, 50th, 75th, and 90th percentiles of the RCs are on average 46.8%, 36.5%, 8.9%, and 20.8% larger during ARs than during non-AR events. This suggests that the runoff response of the basins is more intense during AR events. Additionally, on average 43% of the AMS flows are linked to AR occurrences, with one quarter of AR events exceeding the 10 year return period. Our analysis shows that the widespread flooding that occurred in January–February 1993 and caused human casualties and economic losses was partially due to the occurrence of ARs. In fact, the 1993 AR-related maximum annual flow had a return period of 65 years.

These results highlight the importance of AR activity on the hydrology of semiarid regions and indicate that ARs not only contribute to the basins water resources, but also are linked to extreme conditions that can lead to severe flooding. Compared with the Pacific West Coast, where ARs are linked to extreme flooding along coastal areas (Neiman et al., 2011; Ralph et al., 2006, 2013), AR landfalls in inland semiarid Arizona are as important for their contribution to general water resources (particularly through snow accumulation) as they are for their extreme characteristics. As is the case in the Sierra Nevada mountains (Guan et al., 2016), ARs in Arizona are linked to large streamflows as result of a rise in the melting line and rain-on-snow processes. However, more in-depth analyses need to be conducted to understand how AR-related changes in rain-on-snow processes relate to extreme flood events in the basins. Streamflow simulations with a physically based hydrological model and analysis of satellite-estimated and gridded snow products will help understand the spatiotemporal mechanisms generating flooding. The impact of warmer atmospheric temperatures due to anthropogenic activities is not addressed in the analysis; therefore, decreases in snow cover are considered solely as they relate to AR events. Finally, further analysis addressing the role of dominant teleconnection patterns such as El Niño Southern Oscillation (ENSO), the Arctic Oscillation (AO), and the Pacific-North American (PNA) need to be conducted.

Acknowledgments
This project was funded by the Department of Interior Southwest Climate Science Center and partially by USDA-ARS. We thank our collaborators City of Peoria, City of Chandler, The White Mountain Apache tribe, The Nature Conservancy, and the Salt River Project for their valuable insights. We thank the comments of three anonymous Reviewers, especially Reviewer 3, that greatly improved the manuscript. SNOTEL data are provided (http://www.wcc.nrcs.usda.gov/snow/). Streamflow data were provided by USGS (https://waterdata.usgs.gov) and VIC fields are provided by (https://www.esrl.noaa.gov/psd/data/gridded/data.livneh.html). MERRA reanalysis are produced by NASA (https://gmao.gsfc.nasa.gov/reanalysis/MERRA/). The list of identified AR events is provided in the supporting information (Table S1).

References

Daly, C., Neilson, R. P., & Phillips, D. L. (1994). A statistical-topographic model for mapping climatological precipitation over mountainous terrain. *Journal of Applied Meteorology*, *33*(2), 140–158. https://doi.org/10.1175/1520-0450(1994)033<0140:ASTMFM>2.0.CO;2

Dettinger, M. D. (2013). Atmospheric rivers as Drought Busters on the U.S. West Coast. *Journal of Hydrometeorology*, *14*(6), 1721–1732. https://doi.org/10.1175/JHM-D-13-02.1

Dettinger, M. D., Ralph, F. M., Das, T., Neiman, P. J., & Cayan, D. R. (2011). Atmospheric rivers, floods and the water resources of California. *Water*, *3*(2), 445–478. https://doi.org/10.3390/w3020445

Falcone, J. A., Carlisle, D. M., Wolock, D. M., & Meador, M. R. (2010). GAGES: A stream gage database for evaluating natural and altered flow conditions in the conterminous United States. *Ecology*, *91*(2), 621–621. https://doi.org/10.1890/09–0889.1

Guan, B., Molotch, N. P., Waliser, D. E., Fetzer, E. J., & Neiman, P. J. (2010). Extreme snowfall events linked to atmospheric rivers and surface air temperature via satellite measurements. *Geophysical Research Letters*, *37*, L20401. https://doi.org/10.1029/2010GL044696

Guan, B., Molotch, N. P., Waliser, D. E., Fetzer, E. J., & Neiman, P. J. (2013). The 2010/2011 snow season in California's Sierra Nevada: Role of atmospheric rivers and modes of large-scale variability. *Water Resources Research*, *49*, 6731–6743. https://doi.org/10.1002/wrcr.20537

Guan, B., Waliser, D. E., Ralph, F. M., Fetzer, E. J., & Neiman, P. J. (2016). Hydrometeorological characteristics of rain-on-snow events associated with atmospheric rivers. *Geophysical Research Letters*, *43*, 2964–2973. https://doi.org/10.1002/2016GL067978

Hawkins, G. A., Vivoni, E. R., Robles-Morua, A., Mascaro, G., Rivera, E., & Dominguez, F. (2015). A climate change projection for summer hydrologic conditions in a semiarid watershed of central Arizona. *Journal of Arid Environments*, *118*, 9–20. https://doi.org/10.1016/j.jaridenv.2015.02.022

House, P. K., & Hirschboeck, K. K. (1997). Hydroclimatological and paleohydrological context of extreme winter flooding in Arizona, 1993. In R. A. Larson & J. E. Slosson (Eds.), *Storm-induced geologic hazards: Case histories from the 1992–1993 winter in Southern California and Arizona*, Reviews in Engineering Geology (Vol. 11, pp. 1–25). Boulder, CO: Geological Society of America.

Hughes, M., Mahoney, K. M., Neiman, P. J., Moore, B. J., Alexander, M., & Ralph, F. M. (2014). The landfall and inland penetration of a flood-producing atmospheric river in Arizona. Part II: Sensitivity of modeled precipitation to terrain height and atmospheric river orientation. *Journal of Hydrometeorology*, *15*(5), 1954–1974. https://doi.org/10.1175/JHM-D-13–0176.1

Lavers, D. A., Allan, R. P., Villarini, G., Lloyd-Hughes, B., Brayshaw, D. J., & Wade, A. J. (2013). Future changes in atmospheric rivers and their implications for winter flooding in Britain. *Environmental Research Letters*, *8*(3), 034010. https://doi.org/10.1088/1748–9326/8/3/034010

Lavers, D. A., Villarini, G., Allan, R. P., Wood, E. F., & Wade, A. J. (2012). The detection of atmospheric rivers in atmospheric reanalyses and their links to British winter floods and the large-scale climatic circulation. *Journal of Geophysical Research*, *117*, D20106. https://doi.org/10.1029/2012JD018027

Livneh, B., & Hoerling, M. P. (2016). The physics of drought in the U.S. Central Great Plains. *Journal of Climate*, *29*(18), 6783–6804. https://doi.org/10.1175/JCLI-D-15–0697.1

Livneh, B., Rosenberg, E. A., Lin, C. Y., Nijssen, B., Mishra, V., Andreadis, K. M., . . . Lettenmaier, D. P. (2013). A long-term hydrologically based dataset of land surface fluxes and states for the conterminous United States: Update and extensions. *Journal of Climate*, *26*(23), 9384–9392. https://doi.org/10.1175/JCLI-D-12-00508.1

Lundquist, J. D., Neiman, P. J., Martner, B., White, A. B., Gottas, D. J., & Ralph, F. M. (2008). Rain versus snow in the Sierra Nevada, California: Comparing Doppler profiling radar and surface observations of melting level. *Journal of Hydrometeorology*, *9*(2), 194–211. https://doi.org/10.1175/2007JHM853.1

Maurer, E. P., Wood, A. W., Adam, J. C., Lettenmaier, D. P., & Nijssen, B. (2002). A long-term hydrologically based dataset of land surface fluxes and states for the conterminous United States. *Journal of Climate*, *15*(22), 3237–3251. https://doi.org/10.1175/1520-0442(2002)015 < 3237:ALTHBD>2.0.CO;2

Neiman, P. J., Ralph, F. M., Moore, B. J., Hughes, M., Mahoney, K. M., Cordeira, J. M., & Dettinger, M. D. (2013). The landfall and inland penetration of a flood-producing atmospheric river in Arizona. Part I: Observed synoptic-scale, orographic, and hydrometeorological characteristics. *Journal of Hydrometeorology*, *14*(2), 460–484. https://doi.org/10.1175/JHM-D-12–0101.1

Neiman, P. J., Schick, L. J., Ralph, F. M., Hughes, M., & Wick, G. A. (2011). Flooding in Western Washington: The connection to atmospheric rivers. *Journal of Hydrometeorology*, *12*(6), 1337–1358. https://doi.org/10.1175/2011JHM1358.1

Ralph, F. M., Coleman, T., Neiman, P. J., Zamora, R. J., & Dettinger, M. D. (2013). Observed impacts of duration and seasonality of atmospheric-river landfalls on soil moisture and runoff in Coastal Northern California. *Journal of Hydrometeorology*, *14*(2), 443–459. https://doi.org/10.1175/JHM-D-12–076.1

Ralph, F. M., Neiman, P. J., Wick, G. A., Gutman, S. I., Dettinger, M. D., Cayan, D. R., & White, A. B. (2006). Flooding on California's Russian river: Role of atmospheric rivers. *Geophysical Research Letters*, *33*, L13801. https://doi.org/10.1029/2006GL026689

Rivera, E. R., Dominguez, F., & Castro, C. L. (2014). Atmospheric rivers and cool season extreme precipitation events in the Verde River Basin of Arizona. *Journal of Hydrometeorology*, *15*(2), 813–829. https://doi.org/10.1175/JHM-D-12–0189.1

Rutz, J. J., & Steenburgh, W. J. (2012). Quantifying the role of atmospheric rivers in the interior western United States. *Atmospheric Science Letters*, *13*(4), 257–261. https://doi.org/10.1002/asl.392

Rutz, J. J., Steenburgh, W. J., & Ralph, F. M. (2014). Climatological characteristics of atmospheric rivers and their inland penetration over the Western United States. *Monthly Weather Review*, *142*(2), 905–921. https://doi.org/10.1175/MWR-D-13–00168.1

Simonit, S., Connors, J. P., Yoo, J., Kinzig, A., & Perrings, C. (2015). The impact of forest thinning on the reliability of water supply in Central Arizona. *PLoS One*, *10*(4), e0121596. https://doi.org/10.1371/journal.pone.0121596

Svoma, B. M. (2011). Trends in snow level elevation in the mountains of central Arizona. *International Journal of Climatology*, *31*(1), 87–94. https://doi.org/10.1002/joc.2062

USGS. (1982). *Guidelines for determining flood flow frequency: Bulletin #17B of the hydrology subcommittee*. USGS.